









## Article

# Removal of Pharmaceuticals from Water Using Laccase Immobilized on Orange Peels Waste-Derived Activated Carbon

Osamah J. Al-sareji <sup>1,2,\*</sup> , Mohammed Alaa Abdulzahra <sup>3</sup> , Thaer Shafi Hussein <sup>3</sup>, Ahmed S. Shlakaa <sup>4</sup>, Mustafa M. Karhib <sup>5</sup>, Mónica Meiczinger <sup>1</sup> , Ruqayah Ali Grmasha <sup>1,2,6</sup> , Raed A. Al-Juboori <sup>7,8,\*</sup> , Viola Somogyi <sup>1</sup> , Endre Domokos <sup>1</sup> , Ibijoke Idowu <sup>9</sup>, Manolia Andredaki <sup>9</sup> and Khalid S. Hashim <sup>9,10</sup> 

- <sup>1</sup> Sustainability Solutions Research Lab, Faculty of Engineering, University of Pannonia, Egyetem Str. 10, H-8200 Veszprém, Hungary; meiczinger.monika@mk.uni-pannon.hu (M.M.); ruqayah.grmasha@unswalumni.com (R.A.G.); somogyi.viola@mk.uni-pannon.hu (V.S.)
- <sup>2</sup> Environmental Research and Studies Center, University of Babylon, Babylon, Al-Hillah 51001, Iraq
- <sup>3</sup> DNA Research Center, University of Babylon, Babylon, Al-Hillah 51001, Iraq
- <sup>4</sup> Medical Physics Department, Hilla University College, Babylon, Al-Hillah 51001, Iraq
- <sup>5</sup> Department of Medical Laboratory Techniques, Al-Mustaqbal University College, Babylon, Al-Hillah 51001, Iraq
- <sup>6</sup> Research Group of Limnology, Center for Natural Science, Faculty of Engineering, University of Pannonia, Egyetem u. 10, H-8200 Veszprém, Hungary
- <sup>7</sup> Water and Environmental Engineering Research Group, Department of Built Environment, Aalto University, P.O. Box 15200, FI-00076 Espoo, Finland
- <sup>8</sup> NYUAD Water Research Center, New York University, Abu Dhabi Campus, Abu Dhabi P.O. Box 129188, United Arab Emirates
- <sup>9</sup> School of Civil Engineering and Built Environment, Liverpool John Moores University, Liverpool L3 2ET, UK; k.s.hashim@ljamu.ac.uk (K.S.H.)
- <sup>10</sup> Department of Environmental Engineering, College of Engineering, University of Babylon, Babylon, Al-Hillah 51001, Iraq
- \* Correspondence: osamah.al-sareji@unswalumni.com (O.J.A.-s.); raed.al-juboori@aalto.fi (R.A.A.-J.)



**Citation:** Al-sareji, O.J.; Abdulzahra, M.A.; Hussein, T.S.; Shlakaa, A.S.; Karhib, M.M.; Meiczinger, M.; Grmasha, R.A.; Al-Juboori, R.A.; Somogyi, V.; Domokos, E.; et al. Removal of Pharmaceuticals from Water Using Laccase Immobilized on Orange Peels Waste-Derived Activated Carbon. *Water* **2023**, *15*, 3437. <https://doi.org/10.3390/w15193437>

Academic Editor: Antonio Panico

Received: 20 August 2023

Revised: 11 September 2023

Accepted: 28 September 2023

Published: 29 September 2023



**Copyright:** © 2023 by the authors. Licensee MDPI, Basel, Switzerland. This article is an open access article distributed under the terms and conditions of the Creative Commons Attribution (CC BY) license (<https://creativecommons.org/licenses/by/4.0/>).

**Abstract:** The ongoing discharge of contaminants into the environment has raised concerns about the potential harm they pose to various organisms. In the framework of eliminating pharmaceutical chemicals from aqueous solutions, enzymatic degradation by laccase is an environmentally friendly option. In this investigation, laccase immobilized on biochar derived from agricultural waste (orange peels, OPs) was used for the first time to remove carbamazepine and diclofenac from aqueous media. Different characterizations, such as Fourier-transform infrared spectroscopy (FTIR), scanning electron microscopy and energy dispersive X-ray spectroscopy (SEM-EDS), X-Ray diffraction (XRD), specific surface area ( $S_{BET}$ ), Boehm titration, proximate and ultimate analysis, as well as the point of zero-charge ( $pH_{PZC}$ ) analysis, were used in this study. The immobilization of laccase results in enhanced stability with respect to storage, temperature, and pH compared to laccase in its free form. The findings showed that the ideal conditions for immobilization were a pH of 4, a temperature of 30 °C, and a laccase concentration of 4.5 mg/mL. These parameters led to an immobilization yield of 63.40%. The stability of laccase immobilized on biochar derived from orange peels (LMOPs) was assessed over a period of 60 days, during which they preserved 60.2% and 47.3% of their initial activities when stored at temperatures of 25 °C and 4 °C, respectively. In contrast, free laccase exhibited lower stability, with only 33.6% and 15.4% of their initial activities maintained under the same storage conditions. Finally, the use of immobilized laccase proved to be effective in eliminating these pollutants in up to five cycles. Upon comparing the two systems, namely LMOPs and modified orange peels (MOPs), it becomes apparent that LMOPs exhibit an estimated 20% improvement in removal efficiency. These results affirmed the viability of activated carbon derived from OPs as a cost-effective option for immobilizing laccase. This approach could potentially be further scaled up to effectively eliminate organic pollutants from water sources.

**Keywords:** carbamazepine; diclofenac; laccase; adsorption; enzyme activity; adsorption cycles

## 1. Introduction

The widespread contamination of aquatic environments with pharmaceutical residues is a matter of concern that presents substantial risks to aquatic creatures [1]. Pharmaceuticals include any medications used by humans or animals, whether prescribed or obtained without a prescription. The widespread use of medicines has been shown to contribute to an extended lifespan and improved quality of life. However, the presence of pharmaceutical pollutants in the environment is frequently found due to insufficient monitoring and regulation in most cases [2]. It is an urgent scientific priority to find eco-friendly methods for removing these harmful substances. A number of techniques, including coagulation/flocculation, membrane technologies, and adsorption, have been utilized for eliminating various contaminants from water [3,4]. Due to its simplicity of application and absence of secondary contamination, adsorption is the most popular among these techniques. Meanwhile, the method of adsorption ultimately encounters limitations due to saturation, and regeneration is required to sustain the system's effectiveness. Thus, researchers have incorporated bioremediation and adsorption for the combined elimination and decomposition of pollutants. The use of biodegradable biomolecules, such as enzymes derived from renewable and highly specialized sources, is now being exploited for this objective [5]. According to studies, oxidative enzymes, such as laccase, have shown an excellent level of efficacy in the biodegradation of a wide range of organic pollutants, including pharmaceutical compounds. This enzymatic process effectively transforms these pollutants into chemicals that are either less harmful or biologically inactive substances [6]. Despite laccases having a potential for pollutant biodegradation, their application in the industry may be challenging due to the complexity of recovering them from the reaction media for additional reuse, as well as temperature and pH instability. To overcome these limitations, laccase is immobilized onto firm support to circumvent these constraints.

Immobilization of laccase involves binding the enzyme to a solid support by covalent bonding, entrapment/encapsulation, cross-linking, as well as adsorption. The most common and straightforward technique for immobilizing laccase is adsorption. In recent years, many materials like bentonite, activated carbon, biochar, metal-organic frameworks (MOFs), and chitosan have been identified as possible carrier materials [7]. Biochar has attracted significant attention because of its large specific surface area, porosity, affordability, and widespread accessibility. In addition, biochar can be modified with alkaline and acidic solutions to improve its efficacy. Activated carbon derived from agricultural wastes is a carbon material with beneficial features, including a high specific surface area, high-load enzyme immobilization, excellent dispersibility, and biocompatibility for stable operation [8].

The orange fruit is widely utilized and is among the most often consumed citrus fruits in the agricultural sector, with an estimated annual production of 72 million tons [9]. Orange peel constituted a substantial portion of this fruit. There were nearly 25 million tons of citrus waste generated worldwide in 2016 [10]. In 2013, the production of this waste stream in the European Union (EU) alone exceeded 10 million tons [9]. The unrestricted dispersal of orange peel waste is regarded as a poor management strategy as it negatively impacts the environmental and socioeconomic dimensions of sustainability. The sustainable bioconversion of orange peel into valuable products, such as adsorbents, offers economic advantages while mitigating the negative environmental impacts associated with landfill decomposition.

Consequently, scientists have placed significant emphasis on the process of synthesizing biochar from agricultural waste and its subsequent use as a support for enzyme immobilization [11]. In a recent study conducted by Imam and co-workers (2021), the researchers conducted an investigation into the process of immobilizing laccase onto the surface of biochar derived from rice straw [12]. The primary aim of their study was to investigate the capacity of the immobilized laccase system to facilitate the biodegradation process of anthracene. The immobilization yield of the laccase was found to be 66%, indicating a significant level of effectiveness. Furthermore, the laccase exhibited a notable level

of stability for up to six cycles, suggesting its potential for prolonged use. Additionally, the laccase retained 40% of its original activity, indicating a considerable degree of functionality. In another study, Ghosh and Ghosh (2019) effectively immobilized laccase obtained from *Aspergillus flavus* PUF5 onto coconut fiber [13]. Remarkably, they were able to retain 80% of the enzyme's original activity even after subjecting it to six cycles of consumption. In a different investigation, the process of immobilizing laccase on wheat straw biochar by adsorption and cross-linking was used to facilitate the removal of 2,4-dichlorophenol (2,4-DCP) from soil, which resulted in enhanced enzymatic stability [14]. For the elimination of diclofenac, Lonappan and collaborators (2018) fixed laccase on biochar from multiple feedstocks, namely pine wood (BCPW), pig manure (BCPM), and almond shell (BCAS) produced under varying pyrolysis conditions [15]. The study revealed that the biochars BCPW, BCPM, and BCAS had specific surface areas of 14.1, 46.1, and 17.0 m<sup>2</sup>/g, respectively. The biochars were characterized by the identification of different surface textures, morphologies, surface chemistry, and functional groups. Furthermore, the researchers demonstrated successful covalent immobilization of laccase, with BCPM emerging as the most efficient support material for immobilization owing to its larger specific surface area. In a different research, biochar obtained from maple (MB) and spruce (SB) was utilized as a support for laccase immobilization and chlorinated biphenyl elimination in wastewater [16]. Fourier-transform infrared spectroscopy (FTIR), scanning electron microscopy (SEM), and specific surface area ( $S_{\text{BET}}$ ) analyses revealed that MB had a honeycomb structure with a specific area of 613.6 m<sup>2</sup>/g and a pore volume of 0.695 cm<sup>3</sup>/g, whereas SB had a specific area of 86.3 m<sup>2</sup>/g and a pore volume of 0.065 cm<sup>3</sup>/g. Maple-based BC demonstrated the highest immobilization yield. The immobilization of laccase onto biochar generated from avocado seeds has been investigated in order to enhance the adsorption and biotransformation of acetaminophen (ACT) [17]. The use of citric acid (C<sub>6</sub>H<sub>8</sub>O<sub>7</sub>) and glutaraldehyde on the surface of biochar led to an increased affinity between the enzyme and substrate. The activity of immobilized laccase remained at 50.7% after undergoing seven cycles of reuse during the biotransformation of acetaminophen. The enzyme that was immobilized also demonstrated storage stability for a period of 30 days at temperatures of 4 °C and 25 °C. During this time, it retained over 90% of its biotransformation of ACT activity.

However, no studies have been conducted on the use of orange peels (OPs) as carriers for laccase immobilization in the context of pharmaceutical removal. Therefore, the objective of this study was to evaluate the efficacy of chemically modified OPs in serving as both carriers for laccase and adsorbents for the removal of emerging compounds, namely diclofenac, and carbamazepine, from water samples. The prevalence of such emergent contaminants in waters and their ability to cause environmental and health concerns led to their selection [18]. In addition, the effect of operating variables, including pHs, temperatures, and laccase concentrations, on the laccase absorptivity of OPs was studied. In addition, the investigation evaluates the stability as well as the activity of laccase on OPs during a variety of operating cycles.

## 2. Methodology

### 2.1. Chemicals

The diclofenac (C<sub>14</sub>H<sub>11</sub>Cl<sub>2</sub>NO<sub>2</sub>), and carbamazepine (C<sub>15</sub>H<sub>12</sub>N<sub>2</sub>O) were purchased from Merck KgaA (Dramstadt, Germany). Mineral acids, as well as *T. versicolor* laccase, were acquired from Sigma Aldrich (Burlington, MA, USA). The ABTS (2,2'-Azino-bis(3-ethylbenzthiazoline-6-sulfonic acid)) was also obtained from Sigma. Other substances were obtained from Sigma-Aldrich unless otherwise specified. With no further purification, these substances and reagents of analytical grade were utilized.

### 2.2. Activated Carbon

OPs were rinsed with deionized water to remove impurities before being dried in an oven at 85 °C for 48 h. Then, OPs were ground to 0.5 and 1 mm in particle size. As described in the literature [12,19], the following procedures were used to acquire activated

carbon through a slight alteration: OPs were subjected to a drying process in an oven set at a temperature of 105 °C for a duration of four hours. Subsequently, the dried peels were transferred to a reactor made of stainless steel, where they were subjected to a heating process. The temperature was gradually increased at a rate of 10 °C/min until it reached 550 °C. The purging gas utilized during the retention of the materials was nitrogen at a flow rate of 150 mL/min for a duration of 30 min. The flow of nitrogen persisted until the temperature fell below 200 °C, subsequent to the closure of the furnace. Subsequently, a total of 1.5 g of carbonized material was mixed with a solution containing 200 mL of 5 M H<sub>2</sub>SO<sub>4</sub> and 5 M HNO<sub>3</sub> in a volumetric ratio of 1:1. The mixture underwent stirring using a magnetic agitator and was subjected to reflux at a temperature of 80 °C for a duration of 6 h. Subsequently, the sample was subjected to a rinsing process using distilled water until it reached the point of neutralization (pH 7). The sample was then dried at 80 °C, and then, the particles were reduced to a size range of 100–125 µm by using mortar and pestle for pulverization. Then, it was preserved in an air-tight container for the following examination. The final product of modified orange peels is termed MOPs.

### 2.3. SEM-EDS, $S_{BET}$ and XRD

Scanning electron microscopy (SEM) in conjunction with energy-dispersive X-ray spectroscopy (EDS) (Model JEOL JIB-4700F with a 3–5 kV accelerating voltage range and a 10 nA current, GENTLEBEAM™ (GB), Tokyo, Japan) was employed for the purposes of morphological study and elemental characterization of the samples. The samples underwent a gold/palladium (Au/Pd) coating process to enhance their conductivity and obtain high-quality images. The surface area ( $S_{BET}$ ) was measured using Micromeritics (3Flex). X-ray powder diffraction (XRD) patterns were acquired with a D/Max 2500 VB+X X-ray diffractometer equipped with Cu (40 kV, 35 mA) (Rigaku, Tokyo, Japan). The diffraction measurements were conducted within the 10–80° (2θ) range.

### 2.4. FTIR and Boehm Titration

The examination of the adsorbent structure modification was conducted using FTIR with a wavenumber range covering from 400 to 4000 cm<sup>−1</sup> and a resolution of 2 cm<sup>−1</sup>. Attenuated total reflection (ATR) was employed by utilizing Nicolet™ iS™ 5 FTIR Spectrometer from Thermo Scientific™, Waltham, MA, USA. For determining functional groups, Boehm titration was utilized [20]. About 1 g of the materials was mixed for 48 h at 25 °C with 50 mL of 0.1 M solutions of NaOH, 0.1 M NaHCO<sub>3</sub>, 0.05 M Na<sub>2</sub>CO<sub>3</sub>, and 0.1 M NaOC<sub>2</sub>H<sub>5</sub>. The suspensions underwent decantation and subsequent filtration. Then, the mixtures were re-titrated with a 0.1 M HCl solution. A similar procedure was used to evaluate the basicity of the adsorbent. A 0.1 M HCl was utilized to soak the sample, and 0.1 M NaOH was employed for the titration. The quantification of acidity on the adsorbent was determined by considering the neutralizing capabilities of NaHCO<sub>3</sub> towards carboxylic groups, Na<sub>2</sub>CO<sub>3</sub> against lactonic and carboxylic groups, and NaOC<sub>2</sub>H<sub>5</sub> towards phenolic, carboxylic, lactonic, and carbonyl groups.

### 2.5. Physical and Chemical Analysis

The analysis of OPs and MOPs was carried out in compliance with the American Society for Testing Materials (ASTM) standards: ASTM D 3174-04 for ash content, ASTM D 3173-03 for moisture content, and ASTM D 3175-07 for the volatile matter. The fixed carbon content was calculated by subtracting the combined values of moisture, ash, and volatile matter from 100%. The carbon, hydrogen, oxygen, nitrogen, and sulfur content of OPs and MOPs was measured using an elemental analyzer Model EA 1108 (manufactured by Carl Erba Instruments, Thermo Scientific, Waltham, MA, USA) in accordance with the ASTM D3176 standard procedure.

## 2.6. $pH_{PZC}$

The point of zero-charge ( $pH_{PZC}$ ) of MOPs was calculated using the pH drift technique [21]. Firstly, the pH of the solutions was set via the addition of either HCl or NaOH (0.1 mol/L) to a range between 2 and 10. The MOPs were thereafter introduced into each solution and securely sealed using parafilm. The suspensions were then subjected to agitation at a speed of 150 rpm for a duration of one day. The pH measurement was conducted after a 24-hour period of pH stabilization. The points of equality between initial pH and final pH were found by analyzing the graphs depicting the change in pH ( $\Delta pH$ ) as a function of starting pH. The determination of the point of zero charge ( $pH_{pzc}$ ) was performed.

## 2.7. Enzyme Assay and Immobilization

The enzymatic activity of laccase was assessed by measuring the conversion of ABTS to ABTS<sup>+</sup> radical. According to the literature [22,23], a solution consisting of 125  $\mu$ L of appropriately diluted laccase was mixed with 375  $\mu$ L of newly made 0.1 mM ABTS (pH 4). The resulting combination was then incubated for a duration of 2 min. At a wavelength of 420 nm, the change in absorbance resulting from the process of ABTS oxidation (molar extinction coefficient  $\epsilon = 3.6 \times 10^4 \text{ M}^{-1}\text{cm}^{-1}$ ) was assessed by spectrophotometry (Shimadzu UV-2450, Tokyo, Japan). One unit of free laccase activity is operationally defined as the amount of laccase enzyme required to facilitate the oxidation of 1  $\mu$ mol of ABTS per minute. The final product after laccase immobilized on modified orange peels (MOPs), denoted as LMOPs. The immobilized activity of this product was determined by incorporating 1 mL of a 0.5 M ABTS solution into the LMOPs (60 mg), incubating it for 2 min, and then centrifuging it (8000 rpm). The measurement of absorbance at a wavelength of 420 nm was used to determine the change in absorbance. The activity of the immobilized enzyme was then quantified and expressed in units per gram (U/g). The enzymatic activity of both free and immobilized laccase was determined using Equations (1) and (2), respectively.

$$\text{LMOPs activity U/g} = (\Delta ab \times Df \times Rv) / (\epsilon \times t \times M_{\text{carrier}}) \quad (1)$$

$$\text{Free laccase activity U/mL} = (\Delta ab \times Df \times Rv) / (\epsilon \times t \times v) \quad (2)$$

In the above equations,  $\Delta ab$  represents the absorbance,  $Rv$  denotes the reaction volume in milliliters (mL),  $Df$  signifies the dilution factor,  $\epsilon$  represents the molar extinction coefficient ( $3.6 \times 10^4 \text{ M}^{-1}\text{cm}^{-1}$ ),  $t$  denotes the reaction time in minutes,  $v$  represents the quantity of laccase in milliliters (mL), and  $M_{\text{carrier}}$  represents the mass of the LMOPs in grams.

For immobilization, 25 mg of MOPs were added to a 2 mL tube containing a known concentration of enzyme. The final volume of the cocktail was maintained at 1 mL, and the mixture was incubated for 5 h to guarantee effective adsorption. Following immobilization, the cocktail was centrifuged at 8000 rpm for 3 min, and the supernatant was analyzed to determine the remaining enzyme activity. Subtracting the residual activity from the initial activity provided the immobilized activity. The final product denoted by LMOPs was rinsed, carefully washed, and air-dried for two days at 25 °C.

## 2.8. pH, Temperature, Laccase Concentration, and Storage Stability

Using relative activity as the evaluation metric, the pH, temperature, laccase concentration, and storage stability of free laccase and LMOPs were investigated, where 100% represents maximal activity. For pH stability, 15 mg LMOPs as well as 50  $\mu$ L free laccase were mixed together in centrifuge tubes, including 3 mL buffer solution (pH ranging between 2 and 7), and kept at ambient temperature and 150 rpm for 2 h. The residual activity of free laccase and LMOPs was then measured. At the optimal pH value, the centrifuge tubes were placed in a water bath with various temperatures (ranging from 10 to 60 °C) to determine thermostability. The laccase experiments matched the pH and temperature experiments, with the exception that the optimal enzyme dosage ranged from 0.5 to 5.0 mg/mL. The storage stability of free laccase and LMOPs was determined by storing them at ambient



temperature (25 °C) and in the refrigerator (4 °C) for two months, as well as assessing residual activity every five days within those corresponding optimal circumstances.

### 2.9. Removal Test and Recyclability

The efficacy of LMOPs in removing pharmaceutical pollutants from an aqueous solution was evaluated in a batch system. About 50 mg of LMOPs were introduced to 20 mL of a contaminant mixture (25 mg/L from each) and stirred at 150 rpm at ambient temperature. Aliquots of supernatant (2 mL) were taken every 15 min, followed by a 24-h sample. As a result, the system reached equilibrium 60 min after analyzing all measurements. On the basis of the initial and final concentrations in the aqueous phase, the removal efficacy was calculated. Milli-Q water was used to wash the LMOPs, and the cycle continues to investigate the number of cycles for pharmaceutical pollutants removal. The effect of the physical removal of pharmaceuticals by MOPs owing to adsorption was investigated as well. This was conducted as LMOPs experiments, but MOPs were used instead and then measured by High-Performance Liquid Chromatography (HPLC) for quantification. The tests were conducted using the Merck-Hitachi D-7000 HPLC system. The system column used in this study was the Zorbax SB-Aq, manufactured by Agilent (Santa Clara, CA, USA). The column had dimensions of 150 mm in length and 4.6 mm in diameter, with a particle size of 5 µm with gradient elution. The volume of the sample that was injected was 10 µL. The mobile phase was composed of two eluents: eluent A, which consisted of 0.1 V/V% trifluoroacetic acid in Milli-Q water, and eluent B, which was methanol. The gradient program entails a mobile phase B composition of 40% from 0 to 1 min, followed by a gradient increase to 100% mobile phase B from 1 to 5 min. The process was sustained for a duration of about eight minutes. Subsequently, the gradient was reverted back to its original state. The flow rate was set at 1 mL/min.

### 2.10. Reusability (ABTS)

Utilizing 2,2-Azino-bis-3-ethylbenzothiazoline-6-sulfonic Acid (ABTS) as a substrate, experiments were conducted to determine the reusability of LMOPs over multiple cycles. At room temperature and a frequency of 150 rpm, a quantity of 100 mg of LMOPs was introduced into a 5 mL buffer solution with a pH of 4. The buffer solution also included 0.5 mM of ABTS. The concentration of converted ABTS<sup>+</sup> in the supernatant layer was monitored after a duration of three minutes of centrifuging the reaction mixture at 5000 rpm to determine the activity of LMOPs. After each cycle with three replicate measurements, LMOPs were subjected to a rinsing process using deionized water in order to remove the substrate. The resulting mixture was then decanted and afterward incubated with a pH 4 solution containing 0.5 mM ABTS. This whole process was repeated six times.

### 2.11. Statistical Analysis

In each experiment conducted in this study, the experimental treatments were triplicates. Error bars depict standard deviations, whereas all values represent the mean. Additionally, blank samples have been utilized in every experiment. The data analysis and visualization were performed using the OriginPro 2019b (64-bit).

## 3. Results and Discussion

### 3.1. Physical and Chemical Properties

Table 1 presents an overview of the characteristics of the raw OPs as well as the biochar samples. These parameters were established using proximate and ultimate investigations. According to the outcomes, the pyrolysis procedure used to convert raw OPs to biochar has significantly decreased the amount of moisture and volatile matter. The amount of volatile matter in the biochar produced from OPs is reduced from 67.43 to 9.63%. The biochar yield is proportional to such a significant reduction in volatile matter. A biomass precursor, such as OPs, often comprises cellulose and hemicellulose. These components undergo devolatilization and decomposition at temperatures of around 200 °C. Additionally, the

precursor contains lignin, which decomposes at temperatures above 500 °C [24]. In the meantime, the pyrolysis process led to a marginal increase in the ash level, indicating the existence of non-volatile and non-combustible constituents. The primary reason for this phenomenon could be attributed to the reduction in the overall mass of the material due to the pyrolysis process, which leads to the volatilization of volatile matter. However, it should be noted that inorganic non-volatile and non-combustible components also persist, hence resulting in an observed rise in ash content [25]. The very stable and condensed carbon structure generated at high pyrolysis temperatures led to a large rise in the percentage of fixed carbon. This could be attributed to the high degree of polymerization and the volatilization of volatile matter [24]. The ultimate analysis of the raw and biochar OPs indicates that the biochar exhibits a higher carbon content (increased by 32.1%) and less hydrogen (decreased by 5.65%) and oxygen (decreased by 39.04%) than the raw OPs. The reduction in hydrogen and oxygen levels observed throughout the process of pyrolysis could be attributed to the elimination of volatile components [26]. The results obtained in this study are consistent with the structural characteristics of OPs reported in previous studies. Ullah and colleagues described the elemental composition of OPs as follows: carbon (45.1%), oxygen (42.3%), hydrogen (8.7%), nitrogen (0.46%), and sulfur (0.55%) [27].

**Table 1.** Properties of raw and biochar orange peels (OPs).

Parameters (%)	OPs (Raw) (Wt%) <sup>a</sup> ± SD <sup>b</sup>	OPs (Biochar) (Wt%) ± SD
Moisture	8.93 ± 0.15	1.72 ± 0.03
Volatile matter	67.43 ± 3.18	9.63 ± 0.08
Ash	5.27 ± 0.11	8.91 ± 0.12
Fixed carbon	29.61 ± 0.48	79.74 ± 2.15
C <sup>c</sup>	46.35 ± 0.71	78.45 ± 1.87
O <sup>d</sup>	43.72 ± 0.46	4.68 ± 0.16
H <sup>e</sup>	7.41 ± 0.61	1.76 ± 0.06
N <sup>f</sup>	1.93 ± 0.08	2.38 ± 0.04
S <sup>g</sup>	0.58 ± 0.04	0.95 ± 0.02
H/C	0.16	0.02
O/C	0.94	0.06
N/C	0.04	0.03
S/C	0.01	0.01

Notes: <sup>a</sup> Weight, <sup>b</sup> Standard deviation, <sup>c</sup> Carbon, <sup>d</sup> Oxygen, <sup>e</sup> Hydrogen, <sup>f</sup> Nitrogen, and <sup>g</sup> Sulfur.

### 3.2. $pH_{pzc}$

The measurement of  $pH_{pzc}$  reveals changes to the surface in terms of the total net charge. The average pH of the MOPs, as depicted in Figure 1, was 4.2 (average values). Below the  $pH_{pzc}$  value, MOPs have a favorable positive surface charge, which enhances the attraction and binding of anions. Additionally, when the  $pH_{pzc}$  value is exceeded, the surface of MOPs acquires a negative charge, therefore, facilitating the adsorption of cations.  $pH_{pzc}$  in this work agrees with the values reported elsewhere. For instance, Nascimento and co-workers [28] have also stated that  $pH_{pzc}$  was 3.9. The slight difference in the  $pH_{pzc}$  could be due to inadequate hydroxyapatite coverage of the material. In addition, it could also be due to various chemical conditions encountered throughout the synthesis process that induce the release of water-soluble compounds from the biomass, which could have previously been adsorbed onto the surface of the MOPs, leading to a  $pH_{pzc}$  shift [29].

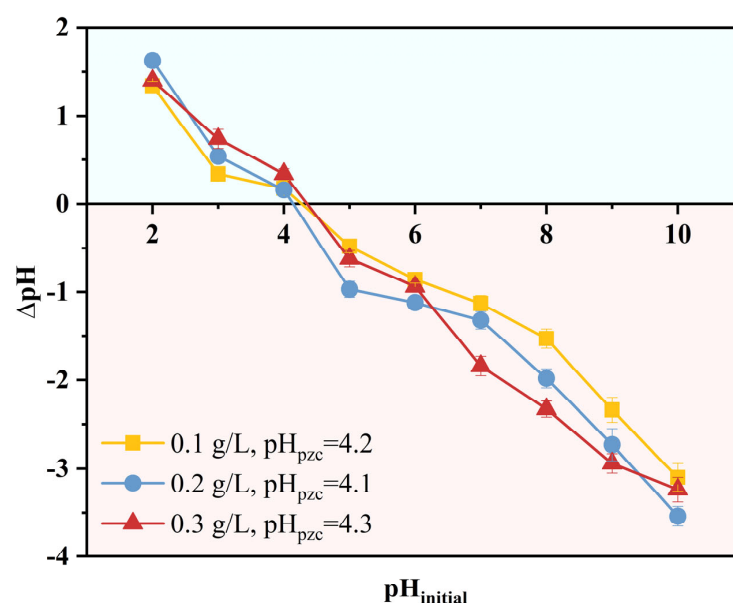


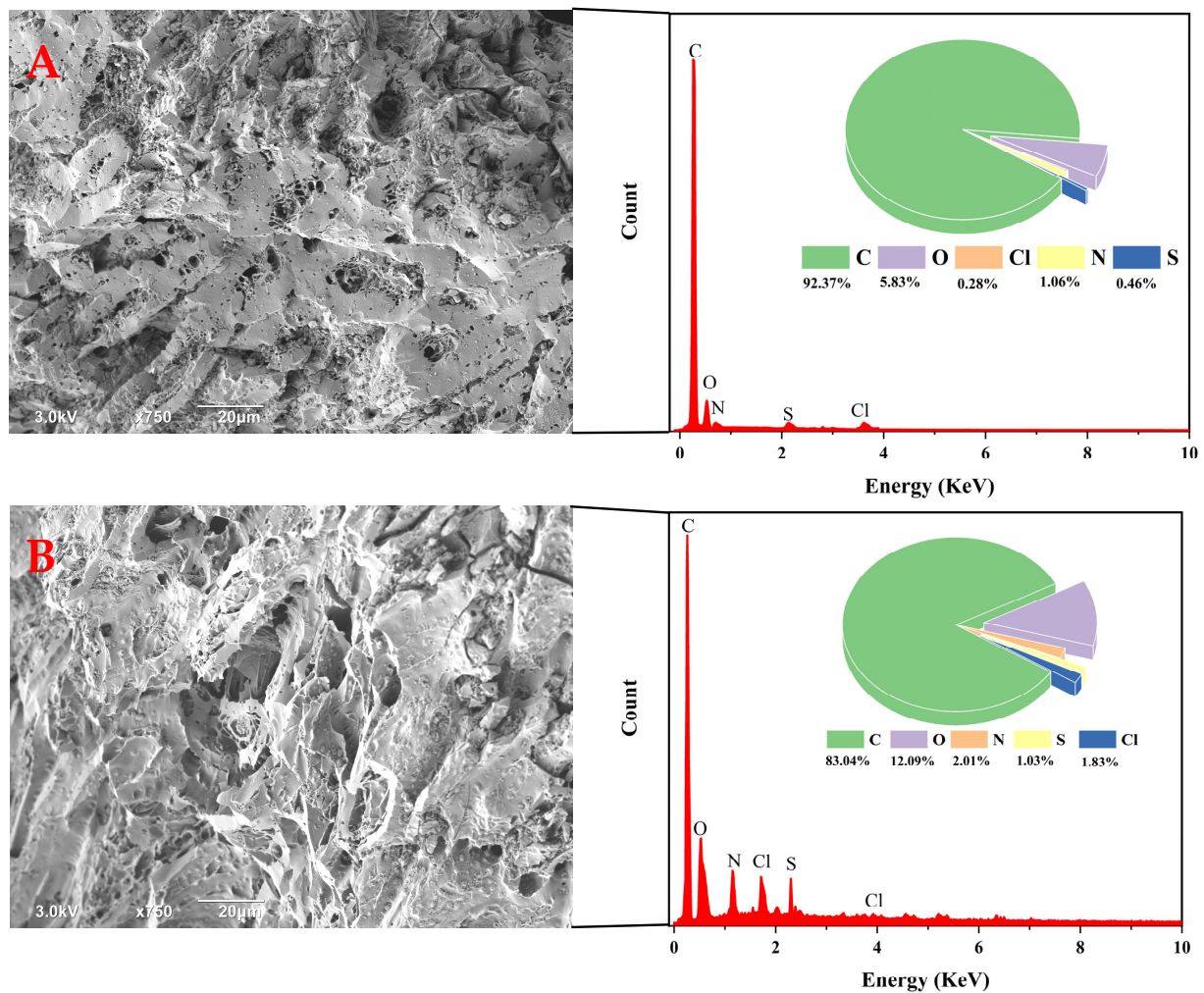
**Figure 1.** Point of zero charge ( $\text{pH}_{\text{pzc}}$ ) plot for modified orange peels (MOPs).

### 3.3. SEM-EDS and XRD

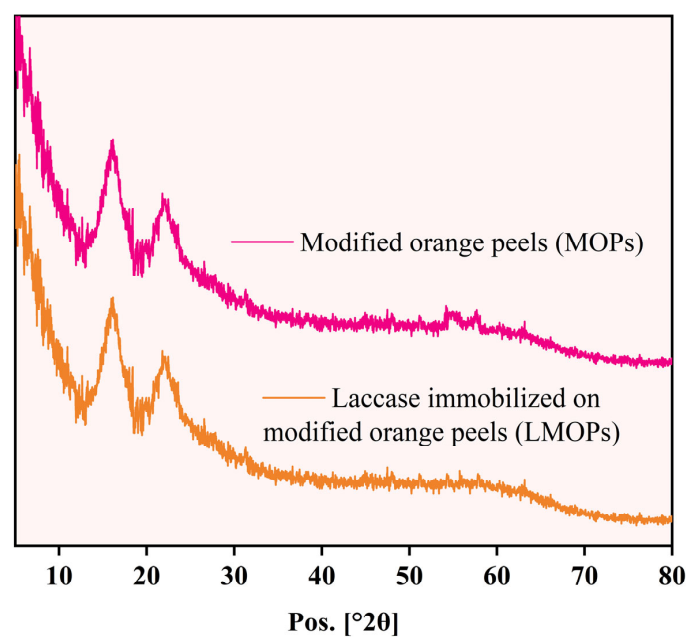
After being treated with an  $\text{H}_2\text{SO}_4/\text{HNO}_3$  mixture, samples of MOPs and LMOPs were analyzed by scanning electron microscopy (SEM) for potential morphological alterations. Figure 2 illustrates the SEM-EDS for MOPs (a) and LMOPs (b). The figure's micrographs reveal that the structural integrity of the samples has not been compromised in any way. The limited level of functional group change on the graphitic structure of biochar under moderate acidic treatment conditions might explain the lack of apparent morphological modifications. After 15 h of treatment with  $\text{HNO}_3$  vapor at  $200^\circ\text{C}$ , Xia and colleagues found no morphological alterations in carbon nanotubes [30]. When laccase was immobilized on biochar to remove toxic malachite green from water, Pandey and co-workers noticed no significant changes in the surface topography, as evidenced by scanning micrographs [22]. In addition, Rosca and co-workers stated that no visual alterations occurred after oxidizing multiwall carbon nanotubes (MWCNTs) in concentrated  $\text{HNO}_3$  for 6 to 9 h. After one day of oxidation, however, fewer nanotubes were observed to have been destroyed [31]. The potential cause of this phenomenon could be attributed to the relatively small dimensions of the laccase protein, ranging from 60 to 90 kilodaltons (kDa), which corresponds to a particle size below five nanometers [15]. Micrographs with a magnification of one micrometer have difficulty capturing this scale. However, EDS results revealed an increase in element N due to the addition of laccase.

Figure 3 displays the X-ray diffraction (XRD) patterns of the MOPs and LMOPs. The significant diffracted peaks seen at  $2\theta = 16.3^\circ$  as well as  $22.3^\circ$  correspond to the (101) and (200) crystallographic planes, respectively, which are characteristic of cellulose. This suggests that the cellulose present in the OPs adsorbent is of the amorphous type I [32].





**Figure 2.** Scanning electron microscopy and energy dispersive X-ray spectroscopy (SEM-EDS) for modified orange peels (MOPs) (A) and laccase immobilized on modified orange peels (LMOPs) (B).



**Figure 3.** X-ray powder diffraction (XRD) spectrum of modified orange peels (MOPs) and laccase immobilized on modified orange peels (LMOPs).

### 3.4. FTIR and Boehm Titration

Figure 4 demonstrates the FTIR for MOPs and LMOPs. The infrared spectra exhibit a wide peak at  $3433\text{ cm}^{-1}$ , which corresponds to the elongation vibration of the O–H bond in MOPs, as reported by Belala et al. (2011) [33]. The vibrational mode detected at a wavelength of  $2920\text{ cm}^{-1}$  is associated with the asymmetric and symmetric stretching of the C–H bonds within cellulose [34,35]. The presence of a peak at around  $1630\text{ cm}^{-1}$  suggests the occurrence of a stretching vibration related to the C=O bond in the carboxylic acid functional groups of xylan, which is a constituent of hemicelluloses [36], which is also suggestive of the amide bond in the laccase protein, confirming its immobilization on the surface of MOPs [37]. The band detected at a wavenumber of  $1260\text{ cm}^{-1}$  corresponds to the vibrational mode associated with the C–O methoxy groups present in lignin. The laccase addition had a very subtle effect on LMOPs, as indicated by the minor increase and expansion of the  $1117\text{ cm}^{-1}$  peak.

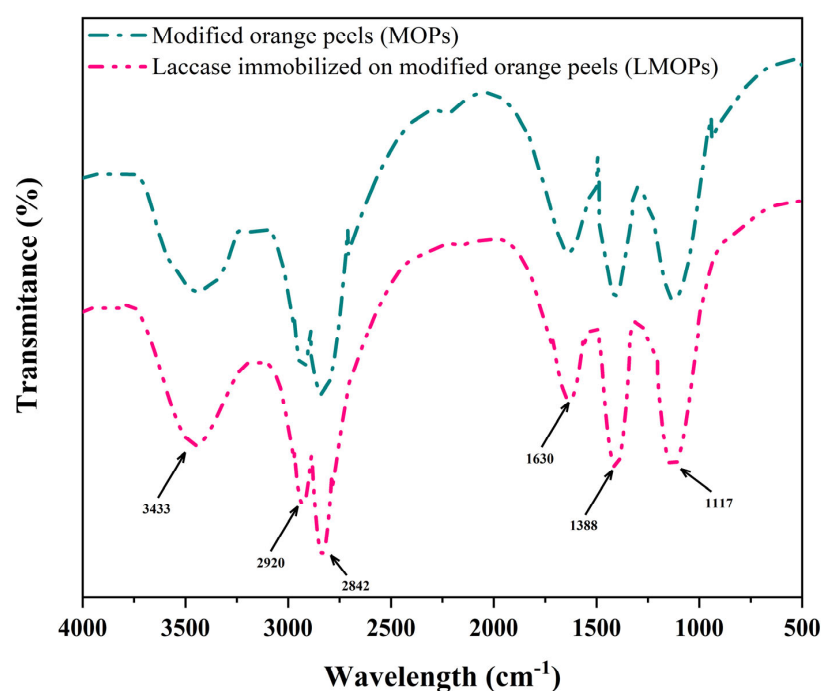


**Figure 4.** Fourier-transform infrared spectroscopy (FTIR) for modified orange peels (MOPs) and laccase immobilized on modified orange peels (LMOPs).

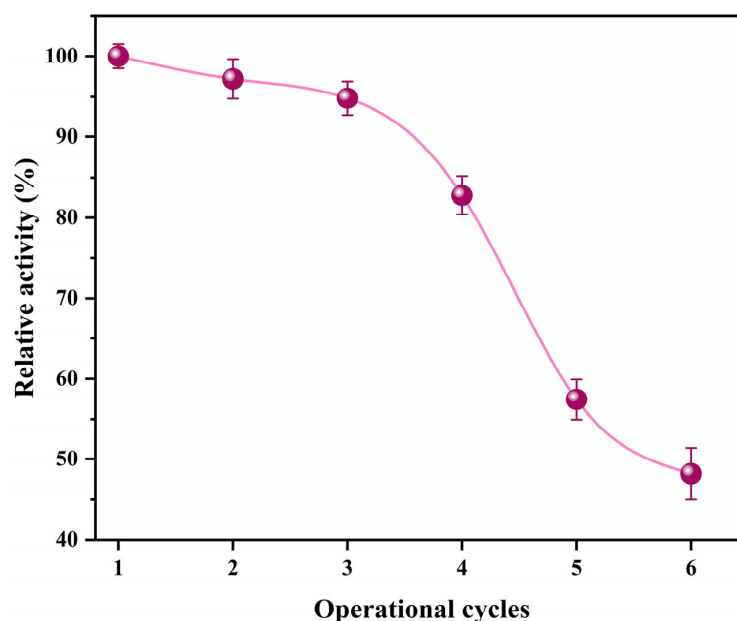
Based on the findings obtained from the Boehm titration, as shown in Table 2, it can be seen that MOPs exhibit a total acidity of 3.56 milliequivalents per gram (meq/g). This overall acidity could be further broken down into specific values for different functional groups within MOPs, namely 0.71 meq/g for carboxylic groups, 1.47 meq/g for carbonyl groups, and 1.38 meq/g for phenolic groups. The surface functional groups for acidic groups increased approximately twofold, while the surface functional groups for basic groups decreased slightly. The increase in value was predicted because of the chemical reaction between acids and the carbon precursor, which led to the formation of more acidic materials during the activation process. The quantitative titration of functional groups with Boehm supports qualitative FTIR findings. The analysis of surface chemistry suggests that acidification is effective in enhancing the surface functional groups of carbon-based materials. The literature has also documented similar observations, whereby the application of mineral acids to the materials resulted in an increase in the acidic group and a reduction in the basic group [38,39].

**Table 2.** Functional groups of the orange peels (OPs) and modified orange peels (MOPs) (meq/g).

Functional Groups	OPs	MOPs
Carbonyl groups	0.52	1.47
Carboxylic groups	0.38	0.71
Phenolic groups	0.96	1.38
Total acidity	1.86	3.56
Total basicity	0.47	0.36

### 3.5. Reusability (ABTS)

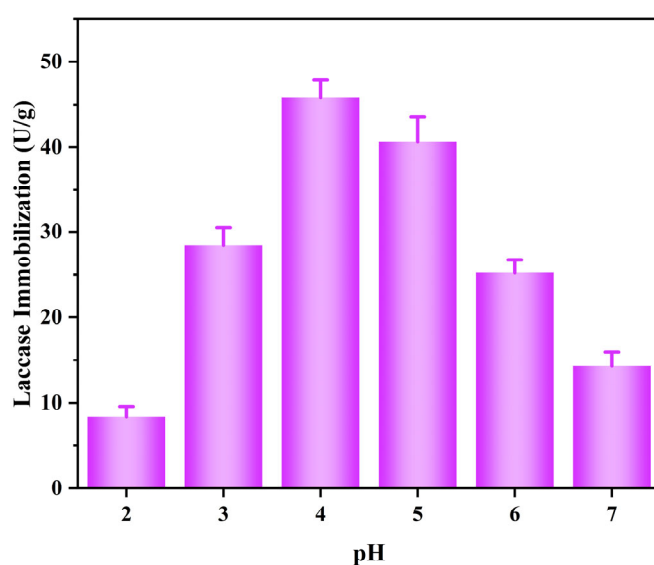
As shown in Figure 5, the residual activity of LMOPs after six regeneration cycles was 48.2% of its initial activity. Even though the relative activity of LMOPs progressively decreased as the number of cycles increased, it stayed higher than 50% after the fifth cycle. The decline in activity seen could be attributed to the disruption of the laccase structure, resulting in its inactivation, as well as the release or detachment of the laccase after repeated washing. Imam and colleagues (2021) used acid-treated rice straw biochar to immobilize laccase and discovered 60% residual activity following six cycles [12]. The reduction in laccase activity was attributed to leaching from the adsorbent throughout rinsing and/or denaturation. Utilizing an orthogonal experimental design, Zheng and co-workers [40] conducted research on the process of immobilizing laccase onto magnetically modified wheat straw biochar by the use of a cross-linking agent (glutaraldehyde) and observed a 22% decrease in activity after five ABTS oxidation cycles.

**Figure 5.** Operational cycles for laccase immobilized on modified orange peels (LMOPs).

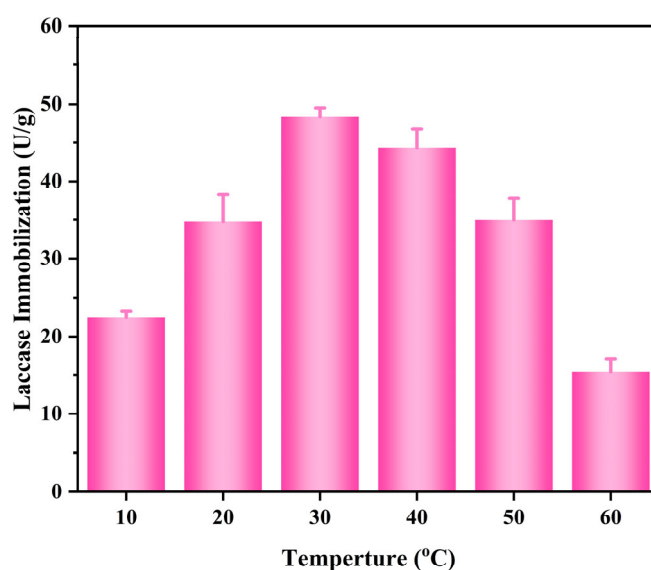
### 3.6. The Optimization of LMOPs Parameters

To reach optimum enzyme immobilization, the pH, temperature, and enzyme concentration were adjusted to optimize the setting. The stability of laccase throughout the immobilization process is significantly influenced by the pH of the solution, thus rendering it a critical factor. Figure 6a,b demonstrates the examined pH range (2 to 7) and temperature range (10 to 60 °C) for LMOPs, respectively. At pH 2, laccase immobilization was low (8.34 U/g) due to a decrease in enzyme activity, while at pH 4, enzyme immobilization was the most effective (45.80 U/g). As the pH value exceeded 4, there was a gradual decline in the immobilization of laccase on LMOPs. Below the isoelectric point of 4.2, which is the average value, the MOPs exhibit a positive net charge. Consequently, this leads to an enhanced electrostatic attraction between the carrier, which carries a positive charge, and

the laccase, which carries a negative charge. As the temperature rises from 10 °C to 30 °C, laccase immobilization is enhanced (from 22.45 to 48.34 U/g), which could be ascribed to the increased rate of enzyme adsorption on MOPs. Following the attainment of the ideal immobilization temperature at 30 °C, the laccase immobilization efficiency experienced a decline to 15.40 U/g when the temperature was raised to 60 °C. This decrease could be attributed to a probable reduction in laccase viability as the temperature increases [14]. As indicated by Figure 6c, the increase of laccase amounts from 0.5 to 5.0 mg/mL resulted in a corresponding elevation in laccase immobilization from 15.31 to 61.30 U/g. However, the immobilization of laccase was unaffected by a further increase in laccase concentration. This could be attributed to the enzyme's capacity to occupy available sites on the MOPs' surface. Thus, the optimal immobilization conditions were found to be pH 4, 30 °C, and 4.5 mg/mL of the enzyme, resulting in an immobilization yield of 63.40% (Figure 6d). The optimal configuration and modification of OPs with copious carbonyl groups led to an increase in immobilization yield [15].

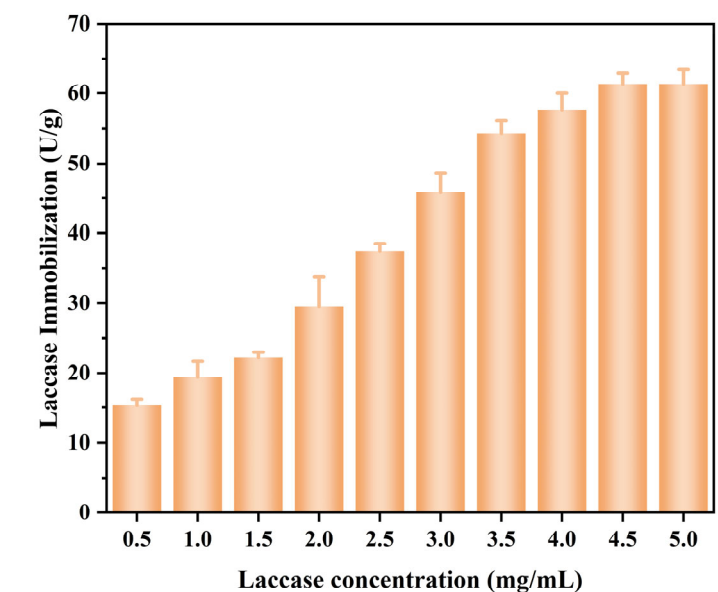


(a)

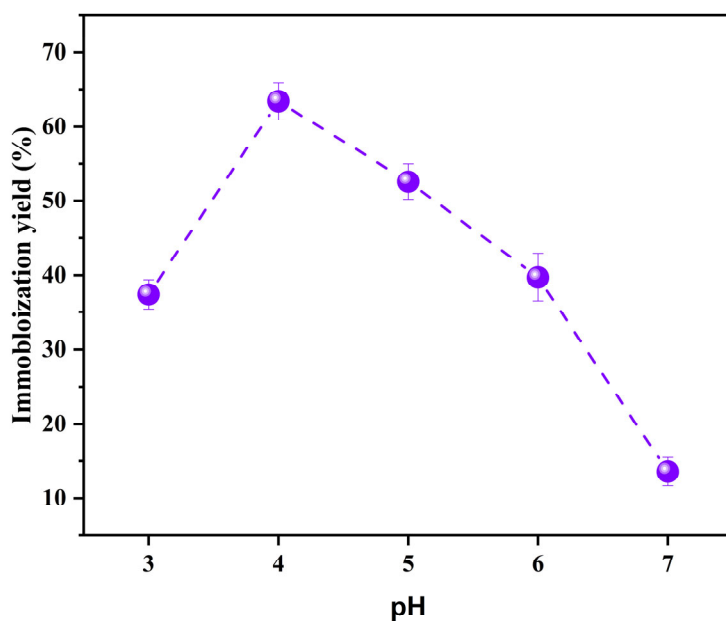


(b)

Figure 6. Cont.



(c)



(d)

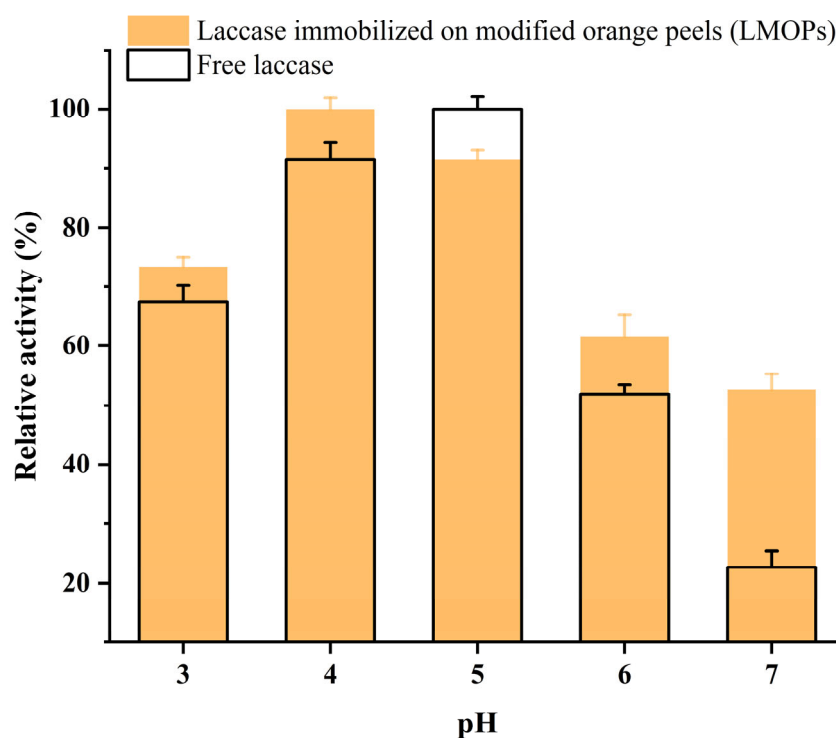
**Figure 6.** The impact of pH (a) and temperature ranges (b), and the laccase concentrations (c) as well as the immobilization yield (d) on the system.

### 3.7. pH, Thermal Stability, and Storage Ability

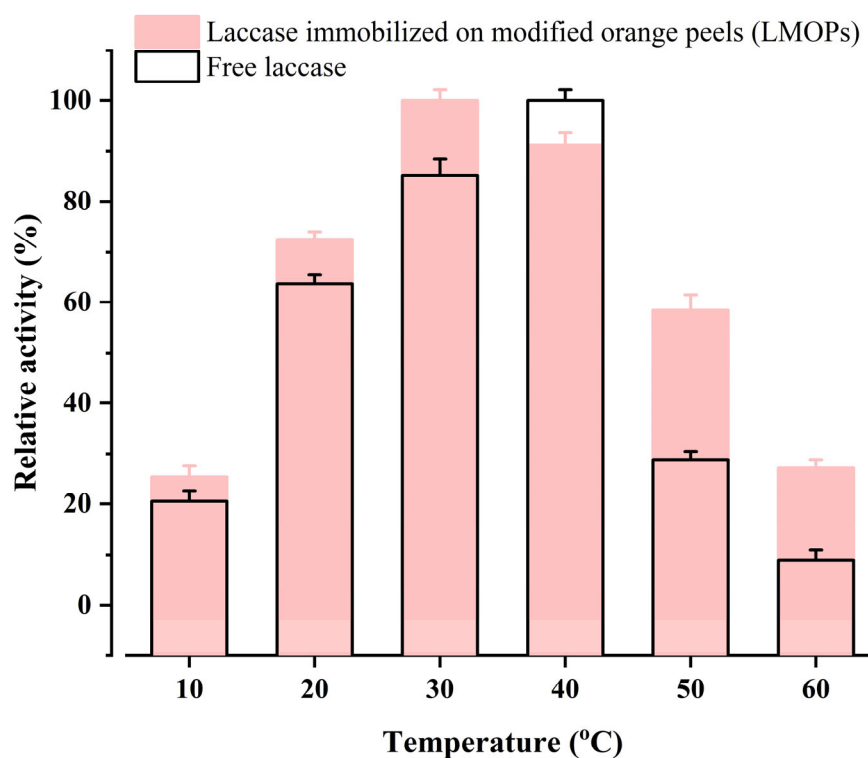
Alterations in pH have the potential to affect the ionization state of amino acids in laccase, thereby exerting an influence on its three-dimensional conformation and functional properties [35,41]. LMOPs exhibited optimal activity at pH 4, whereas free laccase activity was greatest at pH 5, Figure 7a. The observed behavior could possibly be attributed to the following factors: The presence of electrostatic contacts resulting from MOPs in the surrounding microenvironment, as well as the release of  $H^+$  and  $OH^-$  ions in solution, are controlled by the interaction between MOPs and amidoxime groups of laccase. Additionally, the immobilization of laccase leads to a reduction in its mobility [37,42,43]. The relative activity of both free laccase and LMOPs exhibited a significant reduction when the pH value



deviated from the optimal pH range. LMOPs exhibited greater environmental adaptability over a wider pH range compared to free laccase.



(a)



(b)

**Figure 7.** Stability of free laccase and laccase immobilized on modified orange peels (LMOPs) with respect to pH (a) and temperature (b).

The optimal temperatures of free laccase and LMOPs were 40 °C and 30 °C, respectively. Figure 7b also reveals that LMOPs maintained 58.4% of the initial activity at higher temperatures (50 °C), whereas free laccase preserved only 28.9% of its initial activity. LMOPs demonstrated decreased temperature sensitivity. The observed phenomenon could be attributed to the chelation interaction occurring between the free laccase and MOPs, which enhances the structural stability of the immobilized enzyme molecules and provides protection against denaturation. Additionally, it could be explained by the rising substrate diffusion rate at higher temperatures [15,44].

The stability of the enzyme as a reaction biocatalyst is of paramount importance in many biotechnological approaches. Denaturation and activity loss of an enzyme, however, are natural processes that occur over time. Fortunately, the immobilization of enzymes on supports has been shown to effectively mitigate the level of enzyme activity loss. Leonowicz et al. [45] found that immobilization typically restricts the mobility of macromolecules and increases their resistance to inactivation. Figure 8 illustrates the residual activity of both free and immobilized laccases that have been maintained at temperatures of 4 °C and 25 °C. After two months, the LMOPs retained over 60.2% and 47.3% of their initial activities for the respective storing temperatures of 25 °C and 4 °C, whereas laccase-free samples maintained only 33.6% and 15.4% of their initial activities. It was found that immobilizing laccase on MOPs increased the biocatalyst's storage stability in comparison to laccase in its free state. This improvement is a result of the fact that enzyme immobilization restricts conformational changes, thereby preventing denaturation and enhancing stability [46]. Wang and colleagues [43] reported that immobilized enzymes through amidoxime linkage retained 50% of their initial activity following 20 days of storing at 4 °C. Furthermore, in a study conducted by Jiang et al., 2005, it was demonstrated that laccase was immobilized onto chitosan microspheres. The researchers found that, even after a storage period of four weeks at a temperature of 4 °C, around 70% of the enzyme's activity was kept. In contrast, the free enzyme exhibited a drop in its initial activity by approximately 30% [47].

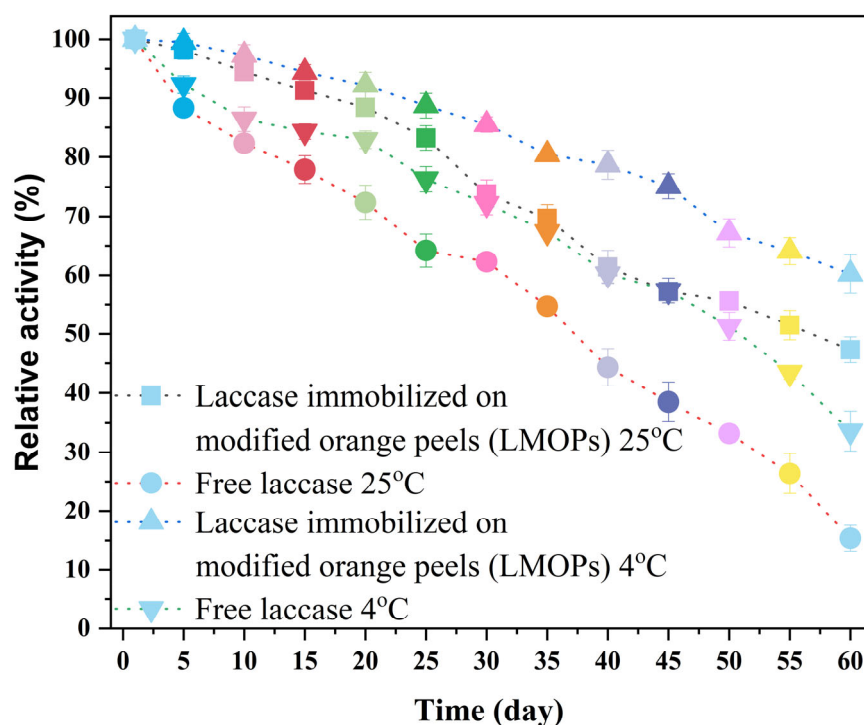


**Figure 8.** Stability of free laccase and laccase immobilized on modified orange peels (LMOPs) at 4 °C and 25 °C.

The findings corresponding to the BET surface area are shown in Table 3, indicating a 16-fold increase in surface area following treatment with acids (22.8 to 367.5 m<sup>2</sup>/g). Impurities are usually eliminated from the surface as well as pores of biochar throughout acid treatment, leading to a rise in surface area and porosity [48]. Following immobilization, the overall reduction in surface area became evident due to the laccase enzyme's occupation of the MOPs' surface area. The findings demonstrate that the laccase remained immobilized on the surface of biochar. Moreover, since biochar had been activated with acid, the laccase occupied a larger surface area, possibly because of enhanced molecular interaction on the surface of MOPs. This increased the interaction with laccase, successfully binding the enzyme. In a similar investigation, Lonappan et al., 2018 found that immobilization of laccase reduced the surface area of biochar by 25–65% [15].

**Table 3.** Specific surface area and pore size of orange peels (OPs), modified orange peels (MOPs), and laccase immobilized on modified orange peels (LMOPs).

	$S_{\text{BET}}$ m <sup>2</sup> /g	$V_{\text{tot}}$	$V_{\text{mic}}$ cm <sup>3</sup> /g	$V_{\text{mes}}$
OPs	22.8	0.047	0.014	0.033
MOPs	367.5	0.103	0.036	0.067
LMOPs	93.4	0.041	0.018	0.023

### 3.8. System Application

LMOPs and MOPs samples were tested in batch mode for up to five cycles, and the results are depicted in Figure 9. For both carbamazepine and diclofenac, the contribution of adsorptive (MOPs) and immobilized-laccase removal (LMOPs) over the course of time was examined. With the LMOPs sample, near-complete elimination occurred over time. It is predicted that a succession of continuous adsorption of both contaminants by MOPs onto vacant sites (sites available after laccase immobilization) could be anticipated. Therefore, the first cycle of adsorption experiments with MOPs revealed removal efficiencies of 73.34% and 82.51% for carbamazepine and diclofenac, respectively. The key factors contributing to the insufficient breakdown of micropollutants are the low oxidative efficiency of laccase and the steric barrier between laccase and the target molecule [49]. Possibly enhanced electron transfer between laccase and contaminants after adsorption on the MOPs surface contributes to the simultaneous and complete removal of both contaminants.

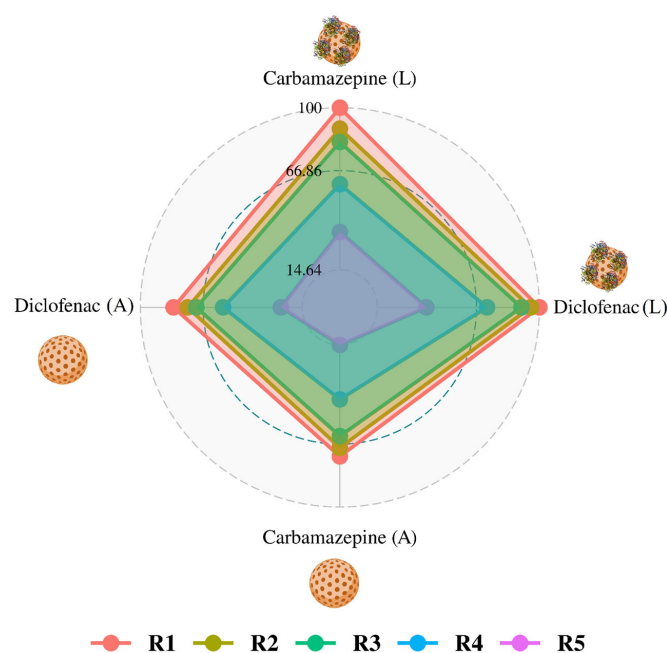


**Figure 9.** The removal percentage of carbamazepine and diclofenac and the long-term performance.

It was noticed that the LMOPs had 81.98% and 90.53% removal percentages for carbamazepine and diclofenac, respectively, after the 3<sup>rd</sup> cycle, whereas a removal percentage of 43.30% and 56.40% for carbamazepine and diclofenac, respectively. By comparison of both systems (LMOPs and MOPs), an approximately 20% increase in removal efficiency for LMOPs could be noticed. This removal efficiency (15 to 20%) was also recorded in the last cycle, confirming the significant improvement upon the addition of laccase.

### 3.9. Biosorbent End-of-Life

Limited studies exist on the concerns of regeneration and reutilization of biosorbents, with a notable absence of discussion on the ultimate disposal of these biosorbents. In the context of the widespread commercial use of biosorbents, it is essential to consider the proper disposal of biosorbents to mitigate any potential adverse impacts.

Disposal procedures for biosorbents include incineration, landfilling, fertilizer, regeneration, and reuse [50]. The first step involves the use of incineration, which is particularly effective due to the high lignin and cellulose content of the biosorbents. This procedure serves to reduce both the volume and mass, thus improving the overall recovery process [51]. The biomass has a larger percentage of carbon and lower oxygen content, which is advantageous for enhancing thermal energy acquisition. Additionally, the levels of sulfur and nitrogen were observed to be very low, indicating that the burning of biomass would result in the production of only small quantities of corrosive and harmful gases. Pyrolysis has the potential to function as a viable method for the retrieval of thermal energy from biomass. The landfill method is an additional cost-effective and straightforward approach for the disposal of waste biosorbents. The desorption of contaminants from biosorbents occurs prior to their disposal in landfills.

Research has also shown that waste adsorbents have the potential to be disposed of by burial in soil or by spreading them across land for natural deterioration, which could potentially be used as a final disposal method [52]. While the cost of the method is very low, the duration required for the natural degradation of adsorbents is much longer. An alternative approach involves the use of waste adsorbents for the purpose of biofertilizer production. The acquisition of raw materials for the production of biosorbents involves the use of microbial sources, as well as the utilization of forestry and agricultural waste, which could include organic compounds that play a crucial role in enhancing soil quality. Therefore, the use of waste adsorbents as biofertilizers not only addresses the issue of proper waste disposal but also contributes to the enhancement of soil structure [53]. A substitute approach to waste disposal involves the immobilization of the waste adsorbent inside an inert substance, which is then sealed. The careful selection of appropriate raw materials for the pretreatment, processing, and ultimate disposal of biosorbents holds considerable importance [54].

The primary objective should be to optimize the effectiveness and capacity of adsorbent materials for the purpose of mitigating environmental contaminants. In order to enhance the rate of adsorption, it is essential to effectively manage the processes of adsorption and desorption, as well as consider the many elements that impact the efficiency of adsorption.

## 4. Limitations

Efficiently conducting comprehensive research is crucial when considering the cost of processing, regeneration, selectivity, and reproducibility in the context of large-scale applications. A systematic examination is also necessary to explore the practical use of orange peel waste materials as adsorbents on a commercial scale. Moreover, it is essential to allocate appropriate attention to both the design and economic aspects in order to achieve effective implementation on an industrial scale. Further study is also essential to investigate the use of purified enzymes in comparison to crude extracts since this could potentially result in a substantial escalation in the expenses associated with biocatalysis. This particular field of inquiry necessitates thorough examination. Additional research is necessary to

explore various combinations of processes in order to develop a dependable and resilient approach to the degradation of micropollutants (transformation products).

## 5. Conclusions

This work explored the immobilization of laccase onto orange peel-activated carbon for pharmaceutical compounds removal from water. FTIR, SEM-EDS, XRD,  $S_{BET}$ , Boehm titration, proximate and ultimate analysis, as well as  $pH_{PZC}$  were utilized for characterizing the produced materials. The immobilization of laccase onto MOPs was evaluated at different temperatures, pH, and laccase concentration with a single variable approach. The immobilized laccase demonstrated enhanced resistance to variations in pH and elevated temperatures, along with increased thermal and storage stability. The immobilized laccase was reusable for up to six cycles, maintaining 48.2% of its initial activity. The efficacy of LMOPs in removing pharmaceutical contaminants from aqueous solution was compared to that of MOPs in the same experimental conditions. LMOPs had better performance compared to MOPs (absorption only). The findings of this study confirm that activated carbon from the agricultural residue (orange peel) could be employed as a low-cost carrier for the immobilization of laccase with the ultimate goal of removing recalcitrant contaminants from water.

**Author Contributions:** Conceptualization, O.J.A.-s., R.A.G., M.M. and R.A.A.-J.; methodology, O.J.A.-s., R.A.G., M.M., R.A.A.-J., M.A.A. and K.S.H.; software, O.J.A.-s. and R.A.G.; validation, I.I., M.A., O.J.A.-s., R.A.G., V.S., E.D. and K.S.H.; formal analysis, O.J.A.-s., R.A.G. and K.S.H.; investigation, O.J.A.-s., R.A.G., M.M., R.A.A.-J. and E.D.; resources, O.J.A.-s., R.A.G., M.M., A.S.S., K.S.H. and V.S.; data curation, O.J.A.-s., R.A.G., M.M. and R.A.A.-J.; writing—original draft preparation, O.J.A.-s., R.A.G., I.I., M.A., K.S.H., M.A.A., A.S.S. and M.M.K.; writing—review and editing, M.A.A., A.S.S., I.I., M.A., K.S.H., R.A.A.-J., T.S.H. and M.M.K.; visualization, O.J.A.-s. and R.A.G. All authors have read and agreed to the published version of the manuscript.

**Funding:** The ÚNKP-23-3-II-PE-12 (Osamah J. Al-sareji) New National Excellence Program of the Ministry for Culture and Innovation from the source of the National Research, Development and Innovation Fund supported this research.

**Data Availability Statement:** The data presented in this study are available on request from the corresponding author.

**Acknowledgments:** The authors express their sincere gratitude for the warm work of the editor and the anonymous reviewers. The views or opinions expressed in this work are attributable to the authors.

**Conflicts of Interest:** The authors declare no conflict of interest.

## References

1. Khan, A.H.; Aziz, H.A.; Khan, N.A.; Hasan, M.A.; Ahmed, S.; Farooqi, I.H.; Dhingra, A.; Vambol, V.; Changani, F.; Yousefi, M.; et al. Impact, disease outbreak and the eco-hazards associated with pharmaceutical residues: A Critical review. *Int. J. Environ. Sci. Technol.* **2021**, *19*, 677–688. [\[CrossRef\]](#)
2. Hawash, H.B.; Moneer, A.A.; Galhoum, A.A.; Elgarahy, A.M.; Mohamed, W.A.; Samy, M.; El-Seedi, H.R.; Gaballah, M.S.; Mubarak, M.F.; Attia, N.F. Occurrence and spatial distribution of pharmaceuticals and personal care products (PPCPs) in the aquatic environment, their characteristics, and adopted legislations. *J. Water Process. Eng.* **2023**, *52*, 103490. [\[CrossRef\]](#)
3. Radovic, S.; Pap, S.; Niemi, L.; Prodanović, J.; Sekulic, M.T. A review on sustainable technologies for pharmaceutical elimination in wastewaters—A ubiquitous problem of modern society. *J. Mol. Liq.* **2023**, *383*, 122121. [\[CrossRef\]](#)
4. Khan, M.D.; Singh, A.; Tabraiz, S.; Sheikh, J. Current perspectives, recent advancements, and efficiencies of various dye-containing wastewater treatment technologies. *J. Water Process. Eng.* **2023**, *53*, 103579. [\[CrossRef\]](#)
5. Al-Sareji, O.J.; Meiczinger, M.; Salman, J.M.; Al-Juboori, R.A.; Hashim, K.S.; Somogyi, V.; Jakab, M. Ketoprofen and aspirin removal by laccase immobilized on date stones. *Chemosphere* **2023**, *311*, 137133. [\[CrossRef\]](#)
6. Bilal, M.; Rasheed, T.; Nabeel, F.; Iqbal, H.M.; Zhao, Y. Hazardous contaminants in the environment and their lac-case-assisted degradation—A review. *J. Environ. Manag.* **2019**, *234*, 253–264. [\[CrossRef\]](#)
7. Dong, C.-D.; Tiwari, A.; Anisha, G.S.; Chen, C.-W.; Singh, A.; Haldar, D.; Patel, A.K.; Singhanian, R.R. Laccase: A potential biocatalyst for pollutant degradation. *Environ. Pollut.* **2023**, *319*, 120999. [\[CrossRef\]](#)



8. Bijoy, G.; Rajeev, R.; Benny, L.; Jose, S.; Varghese, A. Enzyme immobilization on biomass-derived carbon materials as a sustainable approach towards environmental applications. *Chemosphere* **2022**, *307*, 135759. [\[CrossRef\]](#)
9. Siddiqui, S.A.; Pahmeyer, M.J.; Assadpour, E.; Jafari, S.M. Extraction and purification of d-limonene from orange peel wastes: Recent advances. *Ind. Crop. Prod.* **2022**, *177*, 114484. [\[CrossRef\]](#)
10. Zema, D.A.; Calabrò, P.S.; Folino, A.; Tamburino, V.; Zappia, G.; Zimbone, S.M. Valorization of citrus processing waste: A review. *Waste Manag.* **2018**, *80*, 252–273. [\[CrossRef\]](#)
11. Kyomuhimbo, H.D.; Brink, H.G. Applications and immobilization strategies of the copper-centred laccase enzyme; a review. *Heliyon* **2023**, *9*, e13156. [\[CrossRef\]](#) [\[PubMed\]](#)
12. Imam, A.; Suman, S.K.; Singh, R.; Vempatapu, B.P.; Ray, A.; Kanaujia, P.K. Application of laccase immobilized rice straw biochar for anthracene degradation. *Environ. Pollut.* **2021**, *268*, 115827. [\[CrossRef\]](#)
13. Ghosh, P.; Ghosh, U. Immobilization of purified fungal laccase on cost effective green coconut fiber and study of its physical and kinetic characteristics in both free and immobilized form. *Curr. Biotechnol.* **2019**, *8*, 3–14. [\[CrossRef\]](#)
14. Wang, Z.; Ren, D.; Zhao, Y.; Huang, C.; Zhang, S.; Zhang, X.; Kang, C.; Deng, Z.; Guo, H. Remediation and improvement of 2,4-dichlorophenol contaminated soil by biochar-immobilized laccase. *Environ. Technol.* **2021**, *42*, 1679–1692. [\[CrossRef\]](#)
15. Lonappan, L.; Liu, Y.; Rouissi, T.; Pourcel, F.; Brar, S.K.; Verma, M.; Surampalli, R.Y. Covalent immobilization of laccase on citric acid functionalized micro-biochars derived from different feedstock and removal of diclofenac. *Chem. Eng. J.* **2018**, *351*, 985–994. [\[CrossRef\]](#)
16. Li, N.; Xia, Q.; Niu, M.; Ping, Q.; Xiao, H. Immobilizing laccase on different species wood biochar to remove the chlorinated biphenyl in wastewater. *Sci. Rep.* **2018**, *8*, 13947. [\[CrossRef\]](#)
17. da Silva, C.K.H.; Polidoro, A.S.; Ruschel, P.M.C.; Thue, P.S.; Jacques, R.A.; Lima, C.; Bussamara, R.; Fernandes, A.N. Laccase covalently immobilized on avocado seed biochar: A high-performance biocatalyst for acetaminophen sorption and biotransformation. *J. Environ. Chem. Eng.* **2022**, *10*, 107731. [\[CrossRef\]](#)
18. Zhang, Y.; Geißen, S.-U.; Gal, C. Carbamazepine and diclofenac: Removal in wastewater treatment plants and occurrence in water bodies. *Chemosphere* **2008**, *73*, 1151–1161. [\[CrossRef\]](#)
19. Chiang, Y.C.; Lin, W.H.; Chang, Y.C. The influence of treatment duration on multi-walled carbon nanotubes functionalized by H<sub>2</sub>SO<sub>4</sub>/HNO<sub>3</sub> oxidation. *Appl. Surf. Sci.* **2011**, *257*, 2401–2410. [\[CrossRef\]](#)
20. Boehm, H. Surface oxides on carbon and their analysis: A critical assessment. *Carbon* **2002**, *40*, 145–149. [\[CrossRef\]](#)
21. Kosmulski, M. *Surface Charging and Points of Zero Charge*; CRC Press: Boca Raton, FL, USA, 2009.
22. Pandey, D.; Daverey, A.; Dutta, K.; Arunachalam, K. Bioremoval of toxic malachite green from water through simultaneous decolorization and degradation using laccase immobilized biochar. *Chemosphere* **2022**, *297*, 134126. [\[CrossRef\]](#)
23. Al-Sareji, O.J.; Meiczinger, M.; Somogyi, V.; Al-Juboori, R.A.; Grmasha, R.A.; Stenger-Kovács, C.; Jakab, M.; Hashim, K.S. Removal of emerging pollutants from water using enzyme-immobilized activated carbon from coconut shell. *J. Environ. Chem. Eng.* **2023**, *11*, 109803. [\[CrossRef\]](#)
24. Tomczyk, A.; Sokołowska, Z.; Boguta, P. Biochar physicochemical properties: Pyrolysis temperature and feedstock kind effects. *Rev. Environ. Sci. Bio/Technol.* **2020**, *19*, 191–215. [\[CrossRef\]](#)
25. Hanif, M.A.; Ibrahim, N.; Dahalan, F.A.; Md Ali, U.F.; Hasan, M.; Azhari, A.W.; Jalil, A.A. Microplastics in facial cleanser: Extraction, identification, potential toxicity, and continuous-flow removal using agricultural waste-based biochar. *Environ. Sci. Pollut. Res.* **2023**, *30*, 60106–60120. [\[CrossRef\]](#)
26. Das, S.K.; Ghosh, G.K.; Avasthe, R.; Sinha, K. Compositional heterogeneity of different biochar: Effect of pyrolysis temperature and feedstocks. *J. Environ. Manag.* **2021**, *278*, 111501. [\[CrossRef\]](#) [\[PubMed\]](#)
27. Ullah, H.; Abbas, Q.; Ali, M.U.; Cheema, A.I.; Yousaf, B.; Rinklebe, J. Synergistic effects of low-/medium-vacuum carbonization on physico-chemical properties and stability characteristics of biochars. *Chem. Eng. J.* **2019**, *373*, 44–57. [\[CrossRef\]](#)
28. Nascimento, G.E.D.; Duarte, M.M.M.B.; Campos, N.F.; Rocha, O.R.S.D.; Silva, V.L.D. Adsorption of azo dyes using peanut hull and orange peel: A comparative study. *Environ. Technol.* **2014**, *35*, 1436–1453. [\[CrossRef\]](#) [\[PubMed\]](#)
29. Scheverin, V.; Horst, M.; Lassalle, V. Novel hydroxyapatite-biomass nanocomposites for fluoride adsorption. *Results Eng.* **2022**, *16*, 100648. [\[CrossRef\]](#)
30. Xia, W.; Jin, C.; Kundu, S.; Muhler, M. A highly efficient gas-phase route for the oxygen functionalization of carbon nanotubes based on nitric acid vapor. *Carbon* **2009**, *47*, 919–922. [\[CrossRef\]](#)
31. Rosca, I.D.; Watari, F.; Uo, M.; Akasaka, T. Oxidation of multiwalled carbon nanotubes by nitric acid. *Carbon* **2005**, *43*, 3124–3131. [\[CrossRef\]](#)
32. Akinhanmi, T.F.; Ofudje, E.A.; Adeogun, A.I.; Aina, P.; Joseph, I.M. Orange peel as low-cost adsorbent in the elimination of Cd (II) ion: Kinetics, isotherm, thermodynamic and optimization evaluations. *Bioresour. Bioprocess.* **2020**, *7*, 1–16. [\[CrossRef\]](#)
33. Belala, Z.; Jeguirim, M.; Belhachemi, M.; Addoun, F.; Trouvé, G. Biosorption of basic dye from aqueous solutions by Date Stones and Palm-Trees Waste: Kinetic, equilibrium and thermodynamic studies. *Desalination* **2011**, *271*, 80–87. [\[CrossRef\]](#)
34. Danish, M.; Hashim, R.; Ibrahim, M.M.; Sulaiman, O. Optimized preparation for large surface area activated carbon from date (*Phoenix dactylifera* L.) stone biomass. *Biomass-Bioenergy* **2014**, *61*, 167–178. [\[CrossRef\]](#)
35. Al-Sareji, O.J.; Meiczinger, M.; Al-Juboori, R.A.; Grmasha, R.A.; Andredaki, M.; Somogyi, V.; Idowu, I.A.; Stenger-Kovács, C.; Jakab, M.; Lengyel, E.; et al. Efficient removal of pharmaceutical contaminants from water and wastewater using immobilized laccase on activated carbon derived from pomegranate peels. *Sci. Rep.* **2023**, *13*, 11933. [\[CrossRef\]](#)

36. Pavan, F.A.; Lima, E.C.; Dias, S.L.; Mazzocato, A.C. Methylene blue biosorption from aqueous solutions by yellow passion fruit waste. *J. Hazard. Mater.* **2008**, *150*, 703–712. [[CrossRef](#)] [[PubMed](#)]
37. Zhang, Y.; Piao, M.; He, L.; Yao, L.; Piao, T.; Liu, Z.; Piao, Y. Immobilization of laccase on magnetically separable biochar for highly efficient removal of bisphenol A in water. *RSC Adv.* **2020**, *10*, 4795–4804. [[CrossRef](#)] [[PubMed](#)]
38. Zhang, G.; Shi, L.; Zhang, Y.; Wei, D.; Yan, T.; Wei, Q.; Du, B. Aerobic granular sludge-derived activated carbon: Mineral acid modification and superior dye adsorption capacity. *RSC Adv.* **2015**, *5*, 25279–25286. [[CrossRef](#)]
39. Marshall, M.W.; Popa-Nita, S.; Shapter, J.G. Measurement of functionalized carbon nanotube carboxylic acid groups using a simple chemical process. *Carbon* **2006**, *44*, 1137–1141. [[CrossRef](#)]
40. Zheng, Z.; Liu, W.; Zhou, Q.; Li, J.; Zeb, A.; Wang, Q.; Lian, Y.; Shi, R.; Wang, J. Effects of co-modified biochar immobilized laccase on remediation and bacterial community of PAHs-contaminated soil. *J. Hazard. Mater.* **2023**, *443*, 130372. [[CrossRef](#)]
41. Wang, Z.; Ren, D.; Yu, H.; Zhang, S.; Zhang, X.; Chen, W. Preparation optimization and stability comparison study of alkali-modified biochar immobilized laccase under multi-immobilization methods. *Biochem. Eng. J.* **2022**, *181*, 108401. [[CrossRef](#)]
42. Taheran, M.; Naghdi, M.; Brar, S.; Knystautas, E.; Verma, M.; Surampalli, R. Degradation of chlortetracycline using immobilized laccase on Polyacrylonitrile-biochar composite nanofibrous membrane. *Sci. Total. Environ.* **2017**, *605*, 315–321. [[CrossRef](#)] [[PubMed](#)]
43. Wang, Q.; Cui, J.; Li, G.; Zhang, J.; Huang, F.; Wei, Q. Laccase Immobilization by Chelated Metal Ion Coordination Chemistry. *Polymers* **2014**, *6*, 2357–2370. [[CrossRef](#)]
44. Wu, E.; Li, Y.; Huang, Q.; Yang, Z.; Wei, A.; Hu, Q. Laccase immobilization on amino-functionalized magnetic metal organic framework for phenolic compound removal. *Chemosphere* **2019**, *233*, 327–335. [[CrossRef](#)]
45. Leonowicz, A.; Sarkar, J.M.; Bollag, J.M. Improvement in stability of an immobilized fungal laccase. *Appl. Microbiol. Biotechnol.* **1988**, *29*, 129–135. [[CrossRef](#)]
46. Feng, Q.; Wei, Q.; Hou, D.; Bi, S.; Wei, A.; Xu, X. Preparation of amidoxime polyacrylonitrile nanofibrous membranes and their applications in enzymatic membrane reactor. *J. Eng. Fibers Fabr.* **2014**, *9*, 155892501400900218. [[CrossRef](#)]
47. Jiang, D.-S.; Long, S.-Y.; Huang, J.; Xiao, H.-Y.; Zhou, J.-Y. Immobilization of *Pycnoporus sanguineus* laccase on magnetic chitosan microspheres. *Biochem. Eng. J.* **2005**, *25*, 15–23. [[CrossRef](#)]
48. Pandey, D.; Daverey, A.; Arunachalam, K. Biochar: Production, properties and emerging role as a support for enzyme immobilization. *J. Clean. Prod.* **2020**, *255*, 120267. [[CrossRef](#)]
49. D’Acunzo, F.; Galli, C. First evidence of catalytic mediation by phenolic compounds in the laccase-induced oxidation of lignin models. *JBIC J. Biol. Inorg. Chem.* **2003**, *270*, 3634–3640. [[CrossRef](#)]
50. Baskar, A.V.; Bolan, N.; Hoang, S.A.; Sooriyakumar, P.; Kumar, M.; Singh, L.; Jasemizad, T.; Padhye, L.P.; Singh, G.; Vinu, A.; et al. Recovery, regeneration and sustainable management of spent adsorbents from wastewater treatment streams: A review. *Sci. Total. Environ.* **2022**, *822*, 153555. [[CrossRef](#)]
51. Fernández-González, R.; Martín-Lara, M.; Moreno, J.; Blázquez, G.; Calero, M. Effective removal of zinc from industrial plating wastewater using hydrolyzed olive cake: Scale-up and preparation of zinc-Based biochar. *J. Clean. Prod.* **2019**, *227*, 634–644. [[CrossRef](#)]
52. Dhillon, G.S.; Rosine, G.M.L.; Kaur, S.; Hegde, K.; Brar, S.K.; Drogui, P.; Verma, M. Novel biomaterials from citric acid fermentation as biosorbents for removal of metals from waste chromated copper arsenate wood leachates. *Int. Biodeterior. Biodegrad.* **2017**, *119*, 147–154. [[CrossRef](#)]
53. Tay, C.-C.; Muda, A.-M.; Abdul-Talib, S.; Ab-Jalil, M.-F.; Othman, N. The half saturation removal approach and mechanism of Lead (II) removal using eco-friendly industrial fish bone meal waste biosorbent. *Clean Technol. Environ. Policy* **2016**, *18*, 541–551. [[CrossRef](#)]
54. Ramrakhiani, L.; Halder, A.; Majumder, A.; Mandal, A.K.; Majumdar, S.; Ghosh, S. Industrial waste derived biosorbent for toxic metal remediation: Mechanism studies and spent biosorbent management. *Chem. Eng. J.* **2017**, *308*, 1048–1064. [[CrossRef](#)]

**Disclaimer/Publisher’s Note:** The statements, opinions and data contained in all publications are solely those of the individual author(s) and contributor(s) and not of MDPI and/or the editor(s). MDPI and/or the editor(s) disclaim responsibility for any injury to people or property resulting from any ideas, methods, instructions or products referred to in the content.